

Proton Acceleration by High-Intensity UV Laser Irradiation with Thin Foils

Eiichi TAKAHASHI, Susumu KATO, Yuji MATSUMOTO and Isao OKUDA

National Institute of Advanced Industrial Science and Technology (AIST), Tsukuba, Ibaraki 305-8568, Japan

(Received 26 March 2008 / Accepted 11 April 2008)

Proton acceleration experiments using an intense ultraviolet laser were conducted for the first time. The laser system produced pulses having energies of up to 750 mJ at a wavelength of 248 nm with a temporal duration of 400 fs. Thin copper foils of 4 μm were used as targets, and the maximum intensity on the target was 1.3×10^{18} W/cm². The highest energy of protons was 700 keV, which was observed when the laser beam was p-polarized and was incident on the target at an angle of 30°. Fast electrons were generated by vacuum heating or resonance absorption because of the polarization dependence. These protons were accelerated in the target normal direction, which is suggestive of the target normal sheath acceleration mechanism (TNSA).

© 2008 The Japan Society of Plasma Science and Nuclear Fusion Research

Keywords: ultraintense laser, energetic electron generation, energetic ion generation, KrF, ultraviolet, TNSA

DOI: 10.1585/pfr.3.024

Using short-pulse, ultrahigh-intensity lasers for generating fast-proton beams by irradiating thin foils is a new area of research, and has opened up applications such as proton radiography [1], radioisotope generators [2, 3], and inertial confinement fusion [4]. An intense laser beam focused onto a thin foil target creates hot electrons that propagate through the target and induce a space-charge field when they exit. Due to this strong static-electric field, protons can be accelerated perpendicular to the target surface, which is the so-called target normal sheath acceleration mechanism (TNSA) [5].

The strength of the sheath electric field depends not only on the temperature but also on the density of hot electrons, according to the model reported in [6]. The temperature of the hot electrons T_e is proportional to $I\lambda^2$ where I and λ are laser intensity and wavelength, during the major generation processes, such as $J \times B$ heating [7] and vacuum heating [8, 9], which may lead to the disadvantage of having to use short-wavelength lasers. However, the short-wavelength lasers may have better laser absorption, and they produce a higher hot-electron density. For example, according to the vacuum heating model in Ref. [10], the rate of laser absorption increases by the formation of an under-dense plasma shelf, where the formation time is $t_{s45^\circ}(fs) = 130(A/Z)^{1/2}\lambda_\mu$, and A , Z , and λ_μ , are the atomic mass, charge, and wavelength in μm , respectively. When the scaling of a short-wavelength laser is considered, a higher absorption rate is expected, particularly for laser pulses of several 100 fs. In addition, the high-density generation of hot electrons is also expected using parametric scattering with an appropriate scale length of interacting plasmas, when using short-wavelength lasers [11].

However, until now, proton acceleration experiments

have only been conducted using infrared lasers, such as Nd:glass lasers at a wavelength of 1.06 μm [12] and Ti:sapphire lasers at a wavelength of 800 nm [13, 14]. In addition, another experiment employed a laser wavelength, which was the second harmonic of an Nd:glass laser where $\lambda = 526$ nm [15]. To the best of our knowledge, no proton acceleration experiments using ultraviolet lasers have been reported. In this rapid communication, we report, for the first time, a successful application of an intense ultra-violet laser for producing proton acceleration.

Fast-protons were produced from a 248-nm-wavelength KrF laser with a 400-fs pulse duration and 750-mJ energy, and were focused using an f/4.5 off-axis parabolic mirror onto a 4- μm -thick copper target. The focal spot (containing 70% of the energy) was 14- μm full-width at half maximum (FWHM), providing a peak intensity of 1.3×10^{18} W/cm². The seed laser pulses were generated using a Ti:sapphire laser operated at a wavelength of 745 nm. The pulses were frequency tripled using nonlinear optical crystals (THG), and amplified through a discharge and an electron beam (e-beam)-pumped KrF laser amplifier, as shown in Fig. 1. The nanosecond contrast of the frequency-tripled pulses was better than our diagnostic limit of 10^8 , due to nonlinear frequency conversion. A $\lambda/2$ wave plate located just after the THG was used to rotate the laser polarization. The transmitted laser energies of s- and p-polarization pulses were confirmed to be the same.

Amplified spontaneous emissions (ASE) were also generated from these KrF amplifiers. The intensity of the ASE from the e-beam amplifier was weak ($< 10^9$ W/cm² on target) because of its large illumination area. The intensity of the ASE from the discharge amplifier was reduced

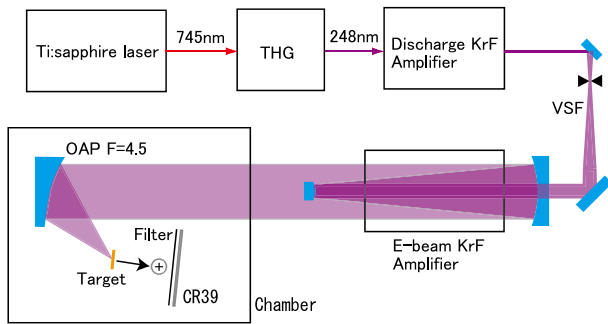


Fig. 1 Illustration of the experimental setup. The Ti:sapphire laser produced the seed laser pulses at a wavelength of 745 nm. The frequency-tripled pulses were amplified using both discharge-pumped and electron-beam-pumped KrF laser amplifiers.

to less than $1 \times 10^{10} \text{ W/cm}^2$ by inserting a vacuum spatial filter (VSF) between the discharge and the e-beam amplifier. In addition, an appropriate discharge time was controlled with respect to the seed laser pulses. CR39 plastic nuclear track detectors were used to observe the accelerated protons. The spatial and spectral distributions of the protons were measured using various filters situated in front of the CR39 plastic detectors, which were placed at the rear of the target and normal to it. A Thomson parabola ion spectrometer was also used to determine the ratio of the atomic mass and charge of the accelerated ions; it was found that the majority of the accelerated particles were protons.

Figure 2 is an image, obtained from the etched CR39 plastic detector, of a proton produced using a p-polarized laser incident at an incident angle of 30° . The position, thickness, and expected proton transmission energy of the filters estimated using the SRIM code [16], are given in the figure caption. The highest energy observed of the fast protons was in the range of 700 to 900 keV, for which an 8- μm aluminum filter is transparent and an 11- μm filter is opaque. The beam divergence angles were 40° for the 700 keV protons and 50° for the 250 keV protons, as indicated in the figure by the broken circular lines.

After counting the number of etched tracks on the CR39 plastic detector, approximately 10^7 protons were found in the 700 to 900 keV energy range. For s-polarized irradiation, a small number of etched tracks were observed only for the Mylar filter position, suggesting that energy of the accelerated protons for s-polarization was around 250 keV. For an incident angle of 14° , protons with energy of 250 keV were also observed for both s- and p-polarizations.

These results were compared with the maximum proton velocity given by the isothermal expansion model [6] as $v_{\text{front}} = 2c_s \ln(\tau + \sqrt{\tau^2 + 1})$, where $\tau = \omega_{\text{pi}} t / \sqrt{2e}$, $c_s = (Zk_b T_e / m_i)^{1/2}$, and $\omega_{\text{pi}} = (n_{e0} Z e^2 / m_i \epsilon_0)^{1/2}$. In this case, it was assumed that the hot-electron temperature was

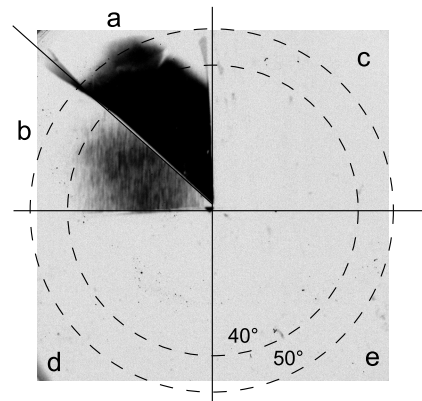


Fig. 2 Proton image obtained from the etched CR39 plastic nuclear track detector. The CR39 was etched in a 6.25 N NaOH solution for 16 hours, maintaining the temperature at 70°C . The filter position, material, and expected proton transmission energy: a: Mylar 2.5 μm ($E > 250 \text{ keV}$), b: Al 8 μm ($E > 700 \text{ keV}$), c: Al 11 μm ($E > 900 \text{ keV}$), d: Al 19 μm ($E > 1250 \text{ keV}$), e: Al 22 μm ($E > 1350 \text{ keV}$). The distance from the target to the CR39 plastic was 5 cm. Etch pits were observed only for the Mylar and Aluminum 8 μm positions.

$T_e = 200 \text{ keV}$, because of the potential transmission energy of the 4- μm -thick copper target. The acceleration time t was assumed to be 500 fs, which was comparable to the laser pulse width. From this assumption, the accelerated proton energy was 700 keV for a hot-electron density of $n_{e0} = 4 \times 10^{19} \text{ cm}^{-3}$. Since the critical density for the KrF laser is $n_c = 1.79 \times 10^{22} \text{ cm}^{-3}$, this density n_{e0} is two orders of magnitude smaller than the maximum electron density for vacuum-heating-produced electrons, which is $n_c/4$. The estimated density of the hot electrons can be explained as a result of the relatively low hot-electron temperature, which was $T_e = 60 \text{ keV}$ for the focused intensity, according to Ref. [10]. Hence, using a thinner target will increase the number of hot electrons that can propagate through the target, and increase the proton energy.

In conclusion, acceleration of protons due to intense ultraviolet laser irradiation of thin foils was observed. The highest proton energy recorded was 700 keV for p-polarization at an incident angle of 30° . This result suggests that the hot electrons were produced by a polarization-dependent mechanism, such as vacuum heating or resonance absorption. Since the direction of the accelerated protons was normal to the target, it is suggested that the TNSA mechanism dominates.

This study was financially supported by the Budget for Nuclear Research of the Ministry of Education, Culture, Sports, Science and Technology, based on the screening and counseling by the Atomic Energy Commission.

- [1] A.J. Mackinnon *et al.*, Phys. Rev. Lett. **97**, 045001 (2006).
- [2] K. Nemoto *et al.* Appl. Phys. Lett. **78**, 595 (2001).

- [3] S. Fritzler *et al.*, Appl. Phys. Lett. **83**, 3039 (2003).
- [4] M. Roth *et al.*, Phys. Rev. Lett. **86**, 436 (2001).
- [5] S.C. Wilks *et al.*, Phys. Plasmas **8**, 542 (2001).
- [6] P. Mora, Phys. Rev. Lett. **90**, 185002 (2003).
- [7] W.L. Kruer *et al.*, Phys. Fluids **28**, 430 (1985).
- [8] F. Brunel, Phys. Rev. Lett. **59**, 52 (1987).
- [9] P. Gibbon *et al.*, Phys. Rev. Lett. **68**, 1535 (1992).
- [10] P. Gibbon, Phys. Rev. Lett. **73**, 664 (1994).
- [11] S. Kato *et al.*, Plasma Fusion Res. **2**, 032 (2007).
- [12] R.A. Snavely *et al.*, Phys. Rev. Lett. **85**, 2945 (2000).
- [13] A.J. Mackinnon *et al.*, Phys. Rev. Lett. **88**, 215006 (2002).
- [14] T. Nayuki *et al.*, J. Appl. Phys. **100**, 043111 (2006).
- [15] A. Maksimchuk *et al.*, Phys. Rev. Lett. **84**, 4108 (2000).
- [16] J.F. Ziegler, <http://www.srim.org/>.